ANALYSIS OF HARDWARE AND SOFTWARE FOR INITIAL DIAGNOSIS OF GASTROINTESTINAL DISEASES

Annotation. In this article, the analysis of hardware and software for initial diagnosis of gastrointestinal diseases is considered. Hardware refers to the analysis of the principle of operation of software, algorithms based on physical models, and algorithms based on artificial intelligence. The results of the analysis obtained in the article were obtained as a result of work carried out in cooperation with the gastroenterology department of the Tashkent Medical Academy and the staff of the department of biomedical engineering, informatics and biophysics.

Keywords: medicine, diseases, hardware and software, diagnosis, artificial intelligence, gastrointestinal diseases.

Nowadays, artificial intelligence has been applied in many fields, and good results can be obtained through it, which can be a clear example in the scientific research works.

Artificial intelligence has now risen to the level of state policy in the Republic of Uzbekistan, as an example of which can be seen through the decisions being made.

Currently, the development of artificial intelligence in all countries of the world is developing thoroughly and rapidly. On the development of artificial intelligence, the decision of the President of the Republic of Uzbekistan Sh. Mirziyoyev "On measures to create conditions for the rapid introduction of artificial intelligence technologies" was adopted, this decision is in accordance with the strategy "Digital Uzbekistan - 2030" [1].

In the field of medicine, digital technologies can be widely used in the diagnosis and treatment of various diseases and at various levels. With the help of digital technologies, it is possible to ease the work of doctors, reduce the human factor, reduce research time and increase efficiency.

At this point, the role of artificial intelligence in the digitization of the medical field is very important. Digitization reduces the human factor in the medical field, i.e. avoids excessive paperwork, the complete medical history of patients is stored in a common database. Through this, knowing the patient's medical history, he acts as an assistant to the doctor to make a correct diagnosis.

An example of this is the diagnostic centers based on the expert system being created by the developed countries of the world. As an example, it is possible to take the expert system introduced by the Italian company BTS [2,21,22].

In this expert system, the diseases of the cardiovascular system of patients and the rehabilitation treatment after various body injuries received after a car accident were introduced (Fig. 1).

1 – picture. SMART DX

An example is the Tsels system, an expert system for the detection and treatment of diseases of the oncology, respiratory system, and endocrine system of the Russian Federation (Fig. 2) [2,19,20].

2 – picture. The principle of operation of the Tcells expert system

Analysis of hardware and software tools.

Field of use: Medicine, medical devices for pre-diagnosis.

Task: increase usability by simplifying the design and reducing the size, expanding the functionality.

The essence of the utility model: A photoelectric device includes an aperture, a lens, a photocell, a light filter, and a light source connected to a current source and optically coupled with the possibility of providing light to a device for placing a test sample placed in series.

According to the results of the study of saliva samples using this device, the value of the photocurrent ratio for patients with a healthy stomach is from 0.3 to 0.5, for patients with a high acid state of the stomach - the K coefficient is higher than 0.5, and the hypoacid state of the stomach is lower than 0.3 for patients with These ratios were then used as test data.

By comparing the test data of photocurrent ratios for the saliva of healthy patients with the data of the saliva of the examined patient, it is possible to make a preliminary express diagnosis for the presence or absence of pathology of the gastrointestinal tract (Fig. 3).

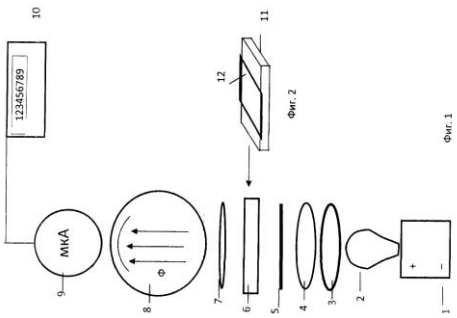

Figure 3. Drawing of the first device.

The hardware components for studying a liquid sample are as follows:

3, 4, - photoelectric device placed in series and optically connected diaphragm,

7 - lens photocurrent

8 - light filter

5 - a built-in current source with the ability to give light

1 - connected light source

2 - includes. and a device for placing the test sample, which is connected to the photocell 8

9 - if equipped with a microammeter,

6 - a device for placing a test sample and a light filter

11 - is made in the form of a removable frame installed between the lenses. 7, wherein the transparent substrate

12 - installed with the possibility of removal.

The device works as follows. The light radiation coming from the light source (bulb) 2 connected to the current source 1 is directed to the guides 3 and focusing diaphragms 4 3,4, then passes through the light filter 5, then the filtered radiation, e.g. green, part of the radiation passes through the substrate 12 with the absorbed saliva sample.

The rest of the radiation through the collecting lens 7 falls on the photocell 8, where the photocurrent is generated. The resulting photocurrent is measured by a microammeter 9 connected to a photocell 8 connected to the display (screen) of the device 10. The obtained result is displayed as a numerical value on screen 10 (for example, 750 μA, 1050 μA).

At the same time, when the device is working, we alternately switch to the filter that transmits red and green color.

According to the theory of turbid media and the laws of light flux absorption, the absorption coefficient of the liquid of the light flux, that is, the decrease in the intensity of light of a certain wavelength transmitted through the liquid, depends on the concentration of this substance in the liquid.

In cases where these light-absorbing elements are of a different nature, for example, depending on the composition of organic and inorganic components, the absorption coefficients differ from each other.

In different samples of saliva, the composition of these elements is different and, accordingly, absorption coefficients are also different [3].

The procedure for conducting research to obtain test data:

1. The device is calibrated, "0" is determined

2. The saliva sample is applied to the surface of the transparent substrate included in the frame and a smear is taken.

3. Switch the device to the red filter, the value of the photocurrent I1 will appear on the screen

4. Switch the device to the green filter, the value of the photocurrent I2 will appear on the screen

5. Calculate the ratio K = I1/I2.

When examining the saliva of patients with a healthy stomach using the proposed device, we found that the value of the K ratio was between 0.3 and 0.5.

When examining the saliva of patients with a hyperacidic state of the stomach, the K ratio value is higher than 0.5, and in patients with a hypoacidic state of the stomach, it is lower than 0.3.

Examples of patient screening include:

Example 1

Patient A., 29 years old.

Gastritis with hyperacidity was revealed in the examination of the stomach.

The saliva sample of this patient was tested by the proposed device. For this, a saliva sample was applied to a transparent substrate embedded in the frame.

First, the saliva sample was screened with a green filter and a value of 855 μA was obtained on the screen. Then checked with a red filter and got a value of 1020 μA. We determined the ratio of these values 855 : 1020 = 0.83.

The comparison with the test data from 0.3 to 0.5 allowed us to conclude that the stomach of the examined patient is hyperacidic, because we know that if the ratio K = I1 / I2 is higher than 0.5, a hyperacidic condition is observed, and if it is lower than 0.3 there will be a hypoacidic state.

Therefore, a value of 0.83 indicates a hyperacid state of the stomach, in which the secretion of gastric juice is higher than normal.

Example 2

Patient V., 52 years old.

The saliva sample of this patient was tested by the proposed device. For this, a saliva sample was applied to a transparent substrate embedded in the frame. First, a green filter was tested through a saliva sample and a photocurrent value of 563 mA

was obtained on the screen. It was then probed with a red filter and obtained a photocurrent value of 1115 μA. We calculated the ratio of the displayed values of photo currents 563 : 1115 = 0.50.

The result shows that this patient does not have gastrointestinal diseases. The proposed device makes it possible to carry out an initial express diagnosis without much effort and to determine whether there are changes in the gastrointestinal tract of the examined person. In this case, a small amount of saliva in the form of a smear applied to the substrate is enough.

But it should be remembered that such diagnostic methods are only indicators. Confirmation of the diagnosis requires a full examination and consultation with a specialist.

If changes are detected compared to the test data, a more accurate examination of the patient is recommended, for example, a stomach examination, fluoroscopy, etc.

Useful model formulation. A part of the electromagnetic radiation falling with the photoelectric effect is reflected from the metal surface, and a part enters the surface layer of the metal, semiconductor or dielectric and is absorbed there. By absorbing a photon, an electron gains energy from it. According to the theory of 1905, based on the law of conservation of energy, when describing light in the form of particles (photons), Einstein's formula for the photoelectric effect is as follows:

$$h\nu = \phi + \frac{mv_m^2}{2}$$

where φ is t. n. work function (minimum energy required to remove an electron from a substance). A is not used in modern scientific literature to designate a work function;

$\frac{mv_m^2}{2}$ — the maximum kinetic energy of the emitted electron;

ν — $h\nu$ frequency of an incident photon with energy;

h — Planck's constant.

This formula shows that there is a red limit of the photoeffect at T = 0 K, that is, the lowest frequency ($h\nu_{min} = \phi$), implies the existence, below which the photon energy does not reach failure [4].

In most substances, the phenomenon is manifested only in ultraviolet radiation, but in some metals (lithium, potassium, sodium) visible light is also sufficient.

A reverse polarity voltage applied to the electrodes reduces the photoelectric current because the electrons have to do extra work to overcome the electrostatic forces.

The minimum voltage that stops the photocurrent completely is called the retarding or blocking voltage.

The maximum kinetic energy of electrons is expressed by the retarding voltage:

$$E_k^{max} = eU_3$$

The photoelectric effect is divided into surface effects, when photoelectrons fly from the surface layer of atoms, and volume effects, when photoelectrons fly from the volume of a solid. The volumetric photoelectric effect is considered in three stages:

In the first stage, the atomic electron goes into an excited state, in the second stage, the electron comes to the surface under the influence of an attractive electric field, in the third stage, if the electron energy is sufficient to overcome the potential, it hits an obstacle on the surface, and then it leaves the solid body. In general, the following formula can be written:

$$h\nu = E_b + E_l + E_{kin} + \phi$$

where E_b— electron binding energy relative to the Fermi level,

E_l— energy loss of the electron on the way to the surface, mainly due to scattering on the crystal lattice;

E_{kin}— kinetic energy of an electron ejected into vacuum.

A photoelectric device for studying a liquid sample is equipped with a light source connected to a current source, an aperture, a lens, a photocell, a light filter and a device for placing the studied sample. equipped with a microammeter connected to the photocurrent, the device for placing the test sample is made in the form of a removable frame installed between the light filter and the lens, in which a transparent substrate is installed with the possibility of removal.

Field of use: Medicine, medical devices for pre-diagnosis.

Task: Early diagnosis of gastroenterological diseases using artificial intelligence algorithm.

The essence of the utility model: Early diagnosis by classification using algorithms based on neural networks and pre-designed data sets.

Random forest performs a selection of rows and columns with a decision tree as the basis. Models h1, h2, h3, h4 are more different from each other due to the choice of columns than using only bags.

As the number of key data (k) increases, the variance decreases. If you decrease k, the variance increases. But the offset remains constant for the entire process. k can be found using cross-validation. [4]

Node implementation in Scikit-learn. For each decision tree, Scikit-learn accepts only two primary nodes (binary tree) and calculates the node importance using the Gini value:

$$n_j^i = w_j C_j - w_{left(j)} C_{left(j)} - w_{right(j)} C_{right(j)}$$

- ni sub(j)= node importance j
- w sub (j) = weighted number of samples reaching node j
- C sub(j) = node impurity value j

- from left (j) = left child node, divided by node j
- from right(j) = child node j from the right split on node j

Then the importance of each object in the decision tree is calculated as follows:

$$fi_i = \frac{\sum_{j:node\ j\ splits\ on\ feature\ i} ni_j}{\sum_{k \in all\ nodes} ni_k}$$

1. fi sub(i)= feature importance i
2. ni sub(j)= node importance j

They can then be normalized to a value between 0 and 1 by dividing by the sum of all feature importance values:

$$normfi_i = \frac{fi_i}{\sum_{j \in all\ features} fi_j}$$

The final feature value at the random forest level is the average of all trees. For each tree, the sum of object importance values is calculated and divided by the total number of trees:

$$RFfi_i = \frac{\sum_{j \in all\ trees} normfi_{ij}}{T}$$

- RFfi sub (i) = feature importance calculated from all trees in the random forest model
- normfi sub(ij) = normalized feature importance for i in tree j
- T = total number of trees

Node implementation in Spark. For each decision treeSpark calculates feature importance by summing the gain in a measure over the number of samples passing through a node:

$$fi_i = \sum_{j:nodes\ j\ splits\ on\ features\ i} s_j C_j$$

- fi sub (i) = feature importance i
- σ sub (j) = number of samples reaching node j
- C sub(j) = node impurity value j

To calculate the final feature importance at the random forest level, first the feature importance for each tree is normalized with respect to the tree:

$$normfi_i = \frac{fi_i}{\sum_{j \in all\ features} fi_j}$$

- normfi sub(i) = normalized object importance i
- fi sub (i) = feature importance i

Then the importance values of objects from each tree are summed and normalized:

$$RFfi_i = \frac{\sum_j norm\ fi_{ij}}{\sum_{j \in all\ features, k \in all\ trees} normfi_{jk}}$$

- RFfi sub (i) = feature importance calculated from all trees in the random forest model
- normfi sub(ij) = normalized feature importance for i in tree j

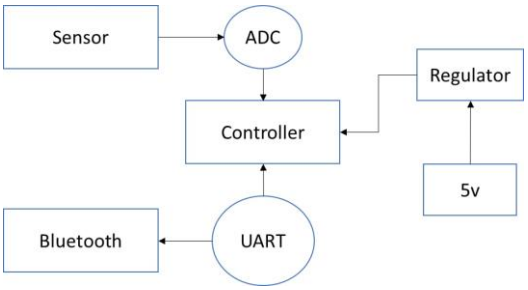

4 - Picture. Drawing of the second "Saliva" device.

ADS1298. ADC(analog-digital converter) is a low-power, multi-channel, 24-bit delta-sigma ADC device developed by Texas Instruments. In the ADS1298 chip, all channels are discretized simultaneously. In addition, the gain parameters of the ADS1298 chip can be adjusted by the built-in program of the PGA amplifier. This chip allows you to measure body temperature, the voltage of an artificial heart pacemaker, to determine whether the sensors are disconnected from the body, to use the RLD circuit [5,6,7]. The data transfer of the chip can reach a speed of 250-32 kb/s (the value of the discrete frequency transmitted per second, 103). Communication between the ECG device and the smartphone is established through the USART interface (Fig. 4). The ADC device also has 4 GPIOs for general use and START pins for synchronous communication with other devices.

Below are the specifications of the ADS1298 analog-digital converter device:

- 8 low-noise PGA and 8 high-precision ADC;
- Channel power: 0.75 mW/channel.
- Noise level: 4 mVPP (150 Hz BW, G = 6).
- Displacement current: 200 pA.
- Data transfer rate: 250 SPS – 32 kSPS.
- Common Mode Rejection: –115 dB.
- Programmable gain: 1, 2, 3, 4, 6, 8, or 12
- ARO' meets the requirements of AAMI EC11, EC13, IEC60601-1, IEC60601-2-27, and IEC60601-2-51 standards.

Provides unipolarity and bipolarity:

- AVDD = 2.7 V - 5.25 V
- DVDD = 1.65 V - 3.6 V
- Built-in RLD amplifier, start detection, WST terminal, speed detection, test signals.
- Integrated respiratory impedance measurement.

- Ability to measure speed digitally.
- Built-in oscillator.
- SPI interface.

Atmega328 microcontroller. The microcontroller receives the primary processed saliva sample signals coming from the ADS1298 chips in the power supply of the saliva device and performs secondary processing and transmits them to the Bluetooth module via the SPI interface. The microcontroller also drives the ADS1298 module, a discrete analog-to-digital saliva sample signal converter and 12-channel device for other peripherals (Figure 4). Communication between the Atmega 328 and external devices was carried out using the SPI module.

The Atmega 328 microcontroller is connected to two SPI interfaces that support high-speed communication with ADS1298 and HC-05 devices. The ADS1298 module provides a serial communication timing system. Synchronization in all communication processes should be at least minimal. A low-power and high-performance Atmega 328 8-bit microcontroller has the following characteristics (Figure 5).

5 – picture. Microcontroller Atmega328.

Below are the specifications of the Atmega328 microcontroller:

• Working with perfect short commands.
• 40 pin AVR.
• 32 kB flash memory.
• 1 KB permanent memory.
• 2 KB RAM.
• The number of input and output contacts are 23.
• Timer: 2 8-bit and 1 16-bit.
• 10-bit 6-channel analog-to-digital converter.
• 6-channel wide pulse modulator.
• Separate oscillator.
• Supports SPI master-slave and I2C mode.
• 20 MHz external oscillator.
• Universal synchronous-asynchronous receiver and transmitter.

Bluetooth HC-05. Bluetooth NS-05, one of the main modules of the ECG device supply, provides the process of wireless data exchange between the smartphone device and the ECG device through the USART interface. The NS-05 module's frequency

band and data transmission channel are ISM compliant, ie 2.4GHz. This intermediate frequency is the radio communication frequency range defined by the radio regulations of the International Telecommunication Union [12,13,14].

Also, this intermediate is specially allocated for scientific research developments in the fields of production, science and medicine. NS-05 module uses EDR method for modulation and demodulation process. The data transfer speed of this module is maximum 2.1 Mbits transmission and 160 kbits reception in asynchronous mode and 1 Mbits reception and transmission speed in synchronous mode. The scheme of the Bluetooth NS-05 module is presented in Figure 6 (Figure 6).

The total size of the information of the 8 channels coming from the ADS1298 device is equal to 224x8 = 224x23=227, that is, 227x50/8 = 838 860 800 or 838 860 800/1024 = 819200 Kbit or 800 Mb. If this value is expressed in 16 number system, it is equal to 800/216 = 0.0122 Mb. The total bandwidth of the Bluetooth NS05 device selected for the design of the ECG device is 2.1 Mbits, which is about 10 times more than that of the ADC device (0.0122 Mb), which is suitable for the current demand [16,17,18].

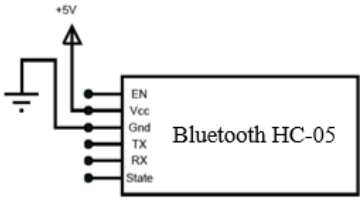

Figure 6. Block diagram of the Bluetooth NS-05 module

Bluetooth NS-05 has two different states (modes): command and transmit/receive states. 38400kbit/s in command mode and 9600kbit/s in data transmission/reception mode.

Below are the specifications of the Bluetooth NS-05 device.

- Chip Bluetooth: HC-05 (BC417143).
- Radio frequency range: 2.4–2.48 GHz.
- Transmission power: 0.25–2.5 mW.
- Signal sensitivity: –80 dBm (0.1% BER).
- Supply voltage: 3.3–5 V.
- Current requirement: 50 mA.
- Radius of influence: up to 10 meters.
- Interface: serial port (UART).
- Mode: master, slave, Master/Slave mode.
- Operating temperature: –25…75 °C.
- Dimensions: 27 x 13 x 2.2 mm.
- Standardized based on IEEE 802.15.1.
- FHSS – radio signal transmission method, modulation type is used.

- The default transmission speed is 38400, but 9600, 19200, 38400, 57600,
- Supports 115200, 230400, 460800 transmission speeds.

An example of a study sample is shown in Table 1. The composition and parameters of the saliva of a healthy patient are shown (Table #1).

KNN and Random Forest algorithms were analyzed, the number of patients in the training sample are 100 and 1000. The obtained results were as expected [9,10,11].

Table #1

parameters of the study sample

Parameters in the study sample	Naming the composition of saliva
Parameter_1	Protein
Parameter_2	Let's go
Parameter_3	Cholesterol
Parameter_4	Glucose
Parameter_5	Ammonium
Parameter_6	Uric acid

For the first time, the process of training a training sample consisting of 100 patients was carried out (Figures 7, 8).

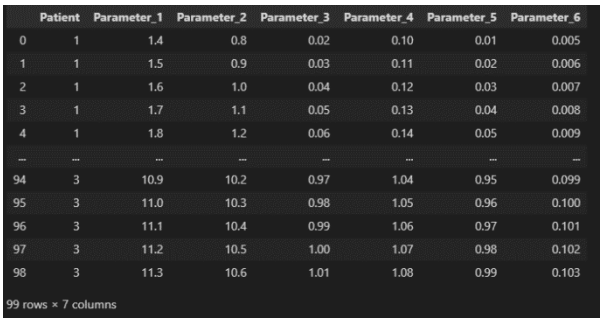

	Patient	Parameter_1	Parameter_2	Parameter_3	Parameter_4	Parameter_5	Parameter_6
0	1	1.4	0.8	0.02	0.10	0.01	0.005
1	1	1.5	0.9	0.03	0.11	0.02	0.006
2	1	1.6	1.0	0.04	0.12	0.03	0.007
3	1	1.7	1.1	0.05	0.13	0.04	0.008
4	1	1.8	1.2	0.06	0.14	0.05	0.009
...	...	...	...	...	...	...	...
94	3	10.9	10.2	0.97	1.04	0.95	0.099
95	3	11.0	10.3	0.98	1.05	0.96	0.100
96	3	11.1	10.4	0.99	1.06	0.97	0.101
97	3	11.2	10.5	1.00	1.07	0.98	0.102
98	3	11.3	10.6	1.01	1.08	0.99	0.103

99 rows × 7 columns

7 - picture. A study sample of 100 patients

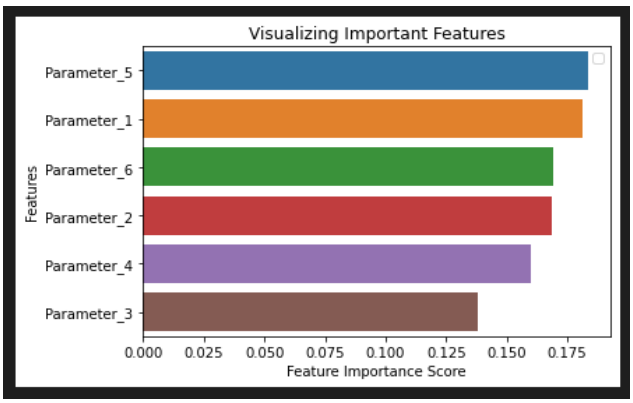

8 – picture. Parameter importance levels (100)

The selected algorithms KNN and Random Forest determined and predicted the importance levels of the parameters (Figure 9).

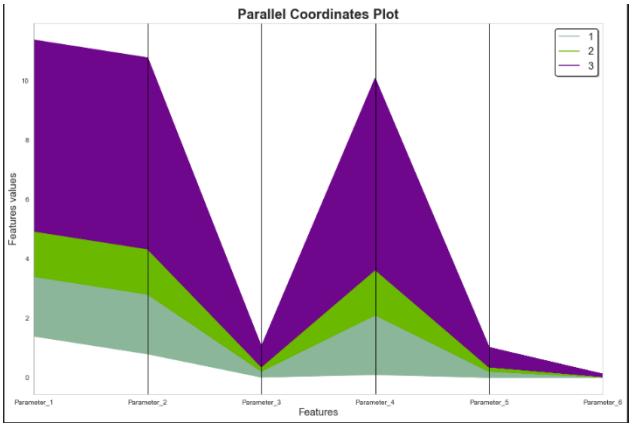

Figure 9. Determination of significance levels of parameters and prediction of disease.

In this algorithm, 3 different color results were obtained during training.

The resulting colors are:

- Black color - the probability of disease is high
- Green - the probability of the disease is low
- Dark green is healthy

In the second process, the training process was carried out on a study sample of 1000 patients. The selected algorithms KNN and Random Forest determined and predicted the importance levels of the parameters (Fig. 10,11).

	Patient	Parameter_1	Parameter_2	Parameter_3	Parameter_4	Parameter_5	Parameter_6
0	1	1.4	0.8	0.02	0.10	0.01	0.005
1	1	1.5	0.9	0.03	0.11	0.02	0.006
2	1	1.6	1.0	0.04	0.12	0.03	0.007
3	1	1.7	1.1	0.05	0.13	0.04	0.008
4	1	1.8	1.2	0.06	0.14	0.05	0.009
...	...	...	...	...	...	...	...
94	3	10.9	10.2	0.97	1.04	0.95	0.099
95	3	11.0	10.3	0.98	1.05	0.96	0.100
96	3	11.1	10.4	0.99	1.06	0.97	0.101
97	3	11.2	10.5	1.00	1.07	0.98	0.102
98	3	11.3	10.6	1.01	1.08	0.99	0.103

99 rows × 7 columns

10 – picture. A study sample of 1000 patients

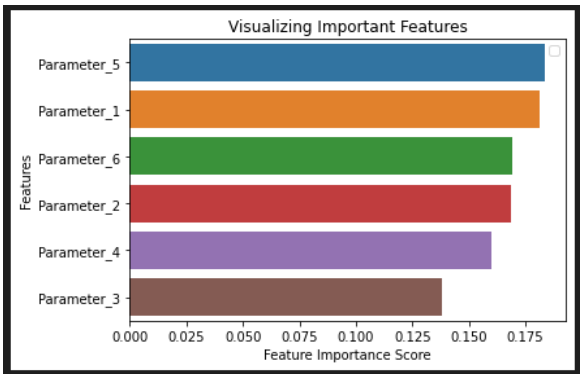

11 - picture. Parameter importance levels (1000)

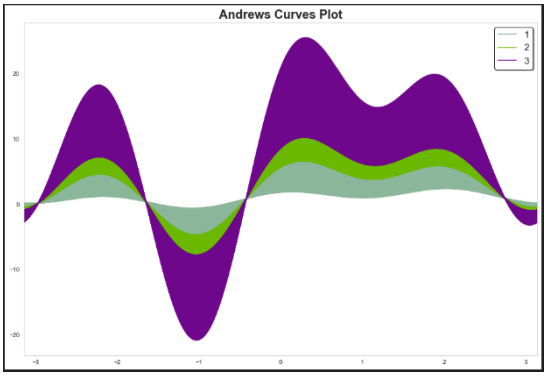

12 - picture. Determination of significance levels of parameters and prediction of disease.

In this algorithm, 3 different color results were obtained during training (Fig. 12). The resulting colors are:

- Black color - the probability of disease is high
- Green - the probability of the disease is low
- Dark green is healthy

Accuracy level of algorithms:

KNN	70% (100)	75% (1000)
Random Forest	75% (100)	84% (1000)

CONCLUSION

In conclusion, the above-mentioned devices provide an opportunity for initial diagnosis of gastrointestinal diseases.

This device is mainly used for preliminary diagnosis as a trial in children and patients who experience discomfort in swallowing the tube.

Devices called "Saliva" are created using the latest technologies, that is, preliminary diagnostics are carried out using algorithms based on neural networks of artificial intelligence.

In the future, we intended to increase the accuracy levels of algorithms based on neural networks.

References

1. http://lex.uz//docs/5297051 O merak po sozdaniyu usloviy dlya uskorennogo innedreniya tekhnologiiy kussstvennogo intellekte
2. Khamzaev J. et al. DRIVER SLEEPINESS DETECTION USING CONVOLUTION NEURAL NETWORK //CENTRAL ASIAN JOURNAL OF EDUCATION AND COMPUTER SCIENCES (CAJECS). - 2022. - T. 1. – no. 4. – S. 31-35.
3. Yakshaboev R. i dr. RAZRABOTKA MODELI RASPOZNAVANIYA GRAFIChESKIX OB'EKTOV NA OSNOVE METHODA «TRANSFER LEARNING» DLYa DIAGNOSTIKI V SPERE ZDRAVOOXRANENII //Conferences. - 2022. - S. 156-164.
4. Yakhaboyev R. DEVELOPMENT OF A SOFTWARE AND HARDWARE COMPLEX FOR PRIMARY DIAGNOSTICS BASED ON DEEP MACHINE LEARNING //CENTRAL ASIAN JOURNAL OF EDUCATION AND COMPUTER SCIENCES (CAJECS). - 2022. - T. 1. – no. 4. – S. 20-24.
5. Yakhaboev R., Bazarbaev M., Ermetov E. PRIMENENIE NEURONNYX SETEY DLYa DIAGNOSTIKI MEDITSINSKIX ZABOLEVANIY //Conferences. - 2022. - S. 148-156.
6. Yakhaboyev R. DEVELOPMENT OF A MODEL OF OBJECT RECOGNITION IN IMAGES BASED ON THE "TRANSFER LEARNING" METHOD //CENTRAL ASIAN JOURNAL OF EDUCATION AND COMPUTER SCIENCES (CAJECS). - 2022. - T. 1. – no. 4. – S. 36-41.
7. Yakshaboev R. E., Ochilov T. D., Siddikov B. N. RAZRABOTKA PROGRAMMNOGO SREDSTVA DLYa IDENTIFIKATsII NOMERNYX ZNAKOV TRANSPORTNYX SREDSTV NA OSNOVE METODOV KOMPUTERNOGO ZRENIya //Journal of new century innovations. - 2022. - T. 15. – no. 1. – S. 81-93.
8. Yakhaboev R., Siddikov B. TsiFROVYE TEXNOLOGII DLYa PERVIChNOY DIAGNOSTIKI RAZNYX MEDITSINSKIX ZABOLEVANIY //Innovations in Technology and Science Education. - 2022. - T. 1. – no. 4. – S. 94-105.
9. Yakshoboyev R., Yakshoboyeva D. ANALYSIS OF ALGORITHMS FOR PREDICTION AND PRELIMINARY DIAGNOSTICS OF

GASTROENTEROLOGICAL DISEASES //CENTRAL ASIAN JOURNAL OF EDUCATION AND COMPUTER SCIENCES (CAJECS). - 2022. - T. 1. – no. 2. - S. 49-56.

10. Djumanov J. et al. Mathematical model and software package for calculating the balance of information flow //2021 International Conference on Information Science and Communications Technologies (ICISCT). – IEEE, 2021. – S. 1-6.
11. Yakhaboyev RE et al. FORECASTING GROUNDWATER EVAPORATION USING MULTIPLE LINEAR REGRESSION //Galaxy International Interdisciplinary Research Journal. - 2021. - T. 9. – no. 12. - S. 1101-1107.
12. Balashova, A. Feyki i roboty: kakimi budut glavnye tekhnologicheskie trendy 2019.
13. A. Balashova, A. Posypkina, E. Balenko // RBK. - 2018. - 3 Dec.
14. Christopher Bishop, Pattern Recognition and Machine Learning, 2006
15. Leon Stenneth, Philip S. Yu, Monitoring and mining GPS traces in transit space, SIAM International Conference on Data Mining
16. Ganesh J., Gupta M., Varma V. Interpretation of Semantic Tweet Representations // arXivpreprint arXiv:1704.00898. - 2017.
17. Zhang A., Culbertson B., Paritosh P. Characterizing Online Discussion Using Coarse Discourse Sequences // Proceedings of the International AAAI Conference on Web and Social Media. — 2017
18. Hastie, T., Tibshirani R., Friedman J. Chapter 15. Random Forests // The Elements of Statistical Learning: Data Mining, Inference, and Prediction. — 2nd ed. - Springer-Verlag, 2009. - 746 p.
19. Stallkamp J. et al. Man vs. computer: Benchmarking machine learning algorithms for traffic sign recognition //Neural networks. - 2012. - T. 32. - S. 323-332
20. Masci J. et al. Stacked convolutional auto-encoders for hierarchical feature extraction //Artificial Neural Networks and Machine Learning-ICANN 2011. - Springer Berlin Heidelberg, 2011. - S. 52-59.
21. Krizhevsky A., Sutskever I., Hinton GE Imagenet classification with deep convolutional neural networks // Advances in neural information processing systems. - 2012. - S. 1097-1105
22. A nanoelectronics-blood-based diagnostic biomarker for myalgic encephalomyelitis/chronic fatigue syndrome (ME/CFS) https://www.pnas.org/doi/full/10.1073/pnas.1901274116
23. Mikaelyan N.P., Komarov O.S., Davydov V.V., Meisner I.S. Biochemistry rotovoy zhidkosti v norme i pri pathology. Educational and methodological assistance for independent work of students of the specialty "Dentistry". - Moscow: IKAR, 2017. - S. 10-11. - 64 p. - ISBN 978-5-7974-0574-0.

24. Human physiology. Textbook. Pod ed. V. M. Pokrovsky, G. F. Korotko. - M.: Medicine, 1997 ISBN 5-225-02693-1 t. 2 c. 39
25. Prives, M.G. Human anatomy / M.G. Prives, N.K. Lysenkov, V.I. Bushkovich. - St. Petersburg: SPbMAPO, 2011, 2014. - 720 p.
26. Human anatomy. V 2 tomax. Volume 1 [Electronic resource]: uchebnik / Pod ed. M.R. Sapina - M. : GEOTAR-Media, 2013. - 528 p.
27. Human anatomy. V 2 tomax. T. II [Electronic resource] : uchebnik / Pod ed. M.R. Sapina - M. : GEOTAR-Media, 2013. - 456 p.:
28. Sinelnikov, R.D. Atlas anatomii cheloveka: v 4 t. / R.D. Sinelnikov. - Moscow: Medicine, 2010.
29. Ostroverkhov G.E. Operative surgery and topographical anatomy [Text]: ucheb. for med. Vuzov / G.E. Ostroverkhov, Yu.M. Bomash, D.N. Lubotsky. - 5-e izd., ispr. - M.: MIA, 2013. - 736 p
30. Topographical anatomy and operative surgery: textbook / A.V. Nikolaev. - 3-e izd., ispr. i dop. - M.: GEOTAR-Media, 2015. - 736 p.
31. R. Nasimov, B. Muminov, S. Mirzahalilov and N. Nasimova, "A New Approach to Classifying Myocardial Infarction and Cardiomyopathy Using Deep Learning," 2020 International Conference on Information Science and Communications Technologies (ICISCT), 2020, pp. 1-5, doi: 10.1109/ICISCT50599.2020.9351386.